

# Schlieren image velocimetry methods for a round, hot, turbulent air-jet

Emilia Georgiana PRISACARIU<sup>\*1,2</sup>, Tudor PRISECARU<sup>2</sup>

\*Corresponding author

<sup>1</sup>COMOTI – Romanian Research & Development Institute for Gas Turbines,  
B-dul Iuliu Maniu 220D, Bucharest 061136, Romania,  
emilia.prisacariu@comoti.ro\*

<sup>2</sup>POLITEHNICA University of Bucharest,  
Splaiul Independentei No.313, Bucharest 060042, Romania,  
tudor.prisecaru@upb.ro

DOI: 10.13111/2066-8201.2023.15.3.6

Received: 12 June 2023/ Accepted: 16 August 2023/ Published: September 2023

Copyright © 2023. Published by INCAS. This is an “open access” article under the CC BY-NC-ND license (<http://creativecommons.org/licenses/by-nc-nd/4.0/>)

**Abstract:** *The present article investigates the accuracy of measurements regarding the velocity profile of a turbulent jet. The measurements are obtained by applying image processing techniques to schlieren methods. The schlieren methods described here are relatively new, having been patented and used for the first time in the last few years. Generally, SIV methods applied to turbulent flows result in unrelatable/ unrelated data, given the path-integrated nature of the flow. The global measurement errors and ways to reduce them are also discussed.*

**Key Words:** BOS, SIV, cross-correlation, PIVlab, kymography

## 1. INTRODUCTION

The results of schlieren image velocimetry methods are almost always presented in comparison with another visualization method, such as PIV. Their accuracy is calculated against a theoretical result or against to data provided by physical sensors. By comparing SIV to the PIV method, for example, one can conclude that the SIV method represents the tracking of real flow elements, while PIV relies on external particles introduced into the flow, and it is assumed that they follow the flow perfectly, as described by [1]. For this reason, Biswas [2] considers the PIV technique to be more of a “synthetic” method. Although PIV defines its workspace as an illuminated plane containing particles that glow when illuminated by a suitable light source, thus providing more accurate data than SIV, which uses path-integrated images, PIV is either impossible or very unlikely to be applied to some types of flows, such as the electrohydrodynamic and compressible flows [3].

SIV experiments on different axisymmetric turbulent flows have been conducted in the past decades, incentivized by the increased computational power available and the new and improved performances of high-speed cameras.

The methods used in the current paper are described firstly by Morales [3] and Settles [4]. The first method is described by Morales as a lagrangian tracking schlieren velocimetry method, using image processing to generate turbulent flow elements boundary distinction and apply a manual tracking method in order to create the path of each element.

This method has been improved by [1], through the automatization of the element tracking process, which resulted in a better measurement accuracy in the jet plume area.

The second method was described by Settles as a “kymograph” method and was first applied to schlieren images with the specific interest of velocity characterization, in [4]. The same method has proven to have a small rise in accuracy when the data resulting from the acquired kymograms was processed in an algorithm that helped distinguish between the central axis velocity curve and other turbulent elements velocity curves.

SIV can also be performed by introducing the results of the lagrangian image pre-processing into commercially available software that uses cross-correlation functions to create the velocity profiles of the flow.

A study of the DC and FFT cross-correlation methods applied in PIVlab [5], is conducted in [6]. The current paper will apply different cross-correlation algorithms with optimized settings provided by PIVlab, and the kymograph method applied to an image sequence containing images of a hot turbulent jet, generated by a hot air gun.

## 2. EXPERIMENTAL SET-UP

The experimental setup consists out of a schlieren Z-type configuration, and a hot air gun mounted in support, placed perpendicular to the schlieren system test area, on a fixed breadboard.

The performances and parameters of the schlieren system are described in Table 1. The experimental setup’s sketch is presented in Figure 1.

Table 1 – Parameters and equipment included into the experimental setup

Type of equipment	Name	Parameters/ Performances
Parabolic twin mirrors	Al-plated, Edmund Optics	Effective focal length= 1524mm
High-speed camera	Phantom Veo 710L CMOS sensor	12-bit per color Resolution: 1280x800 Acquisition speed: 23fps
Knife edge	Black, anti-reflective coating	Vertical positioning, 50% cut-off
Hot air gun	Black & Decker KX1650	Temperature: 450°C Air mass flow: 740 l/min
Light source	LS-W1	Laser pumped, 500mW Optical fibre, round, 1mm diameter

The light source from the optical fiber, placed in the first parabolic mirror’s focal length hit the first parabolic mirror and is spread uniformly over its entire area. The light is collimated between the two parabolic mirrors and exits the second parabolic mirror, landing on a knife edge place at the focal point of the second parabolic mirror.

After the knife edge plane, in its immediate vicinity, the CMOS sensor is placed, imaging the test area as the image of the parabolic mirror fully illuminated.

As presented in Figure 1 and specified in literature [7],  $\alpha$  represents the parabolic mirror off-axis angle, recommended in general to be equal to 3°, but in practice, it can reach up to 15°, depending on the maximum optical errors and optical deviations allowed by the type of investigation conducted.

In this case, a  $\alpha = 9^\circ$ , which allowed the placing of the knife-edge without the coma effect influencing the possibility of applying the required cut-off.

The 50% cut-off was applied relying on literature recommendations, such as [7] and [8], and also on the pre-experiment images recorded.

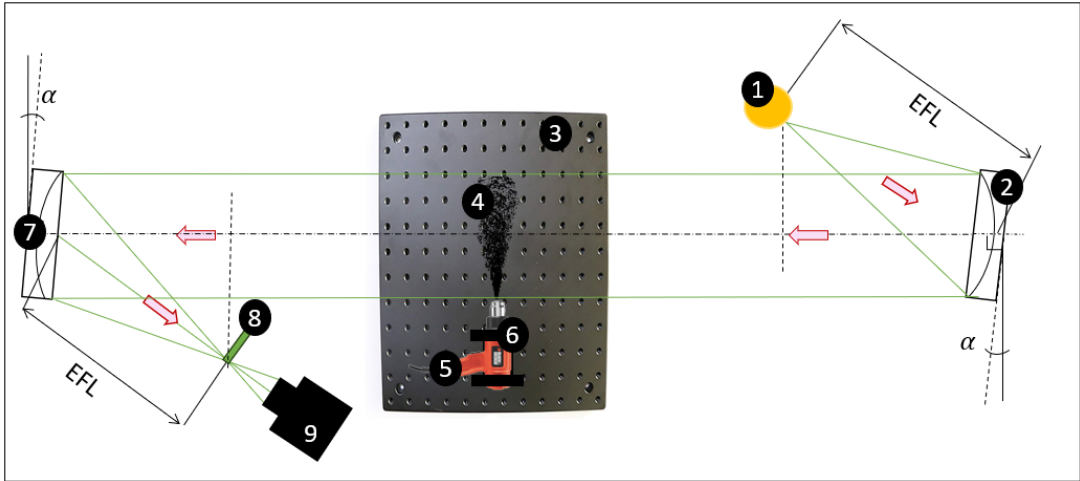


Fig. 1 Experimental setup: 1- light source, 2- first parabolic mirror, 3- fixed breadboard, 4- investigated hot air jet, 5- hot air gun, 6- hot air gun fixed support, 7- second parabolic mirror, 8- vertical knife edge, 9- CMOS sensor (high speed camera)

The pre-experimental campaign had the following objectives: to help obtaining the best ratio between the system sensitivity and the method requirements and to provide an insight into the necessary parameters of the equipment.

The image of the turbulent jet obtained at 80% pre-test cut-off and the sequence of images at 50% cut-off can be observed in Figure 2 and Figure 3, respectively.

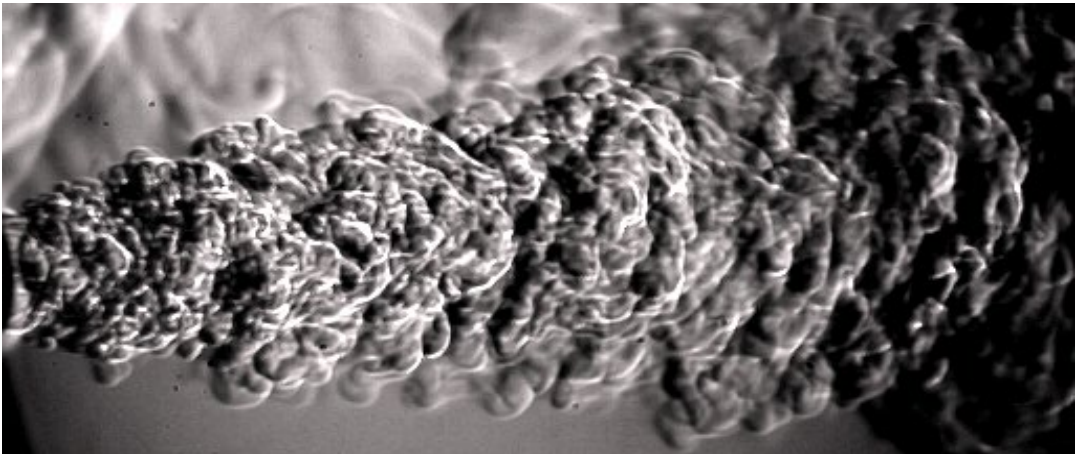


Fig. 2 Schlieren image of the investigated hot air jet, with 80% cut-off

Figure 2 presents images of the jet acquired with an 80% cut-off, meaning that the knife edge blocks 80% of the light source image.

Despite describing the evolution of the jet with most details, it also pictures very intense natural convection elements, which makes it difficult for the algorithm of the SIV methods to differentiate between jet and background.

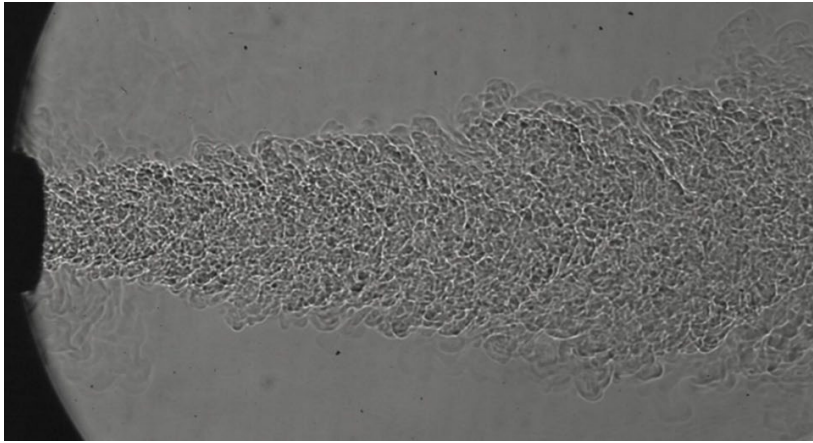


Fig. 3 Schlieren image from the image sequence analyzed, with 50% cut-off

### 3. METHOD IMPLEMENTATION

The first method implemented on the hot-air, turbulent jet is applying a cross-correlation algorithm provided by PIVlab. This method is close to the method used by Morales [3] only in that it tracks the “eddies” formed in the turbulent jet, but without applying other pre-processing techniques. The pre-processing technique applied by Morales introduces an error by describing the elements in black and white, not allowing any sub-pixel interpolation.

The images of the jet should be acquired by using the entire length of the available test area, creating a clearer image of the jet, and reducing any errors which may appear in the tracking mechanism, related to poor image resolution. The settings of the PIVlab session are included in Table 2. After the images are acquired, the image batch is opened into the PIVlab software. PIVlab currently runs as an app, available in Matlab, and is characterized as a free source code, not requiring another license except the one needed for running Matlab. The SIV analysis can be conducted on 2 or more images, depending on the required outcome. Larger image sequences can contribute significantly to lowering the average velocity values obtained.

PIVlab returns data regarding several parameters for the analyzed flow, the one targeted in this paper being the velocity magnitude. Results regarding U and V velocity, vorticity maps, sample shear rate, sample strain rate, resulted vectors and the jet’s streamlines are also presented, but not analyzed as a cross-investigation regarding those parameters cannot be achieved without additional measurements.

Table 2 – Parameters applied in the PIVlab session

PIV algorithm deployed	FFT window deformation
Sub-pixel estimator	Gauss 2x3 - point
Interrogation area	64x32
Interrogation steps	32X16 16X8
Correlation robustness	Standard
Calibration process	x- increases towards right y – increases towards top
ROI selected	to contain the jet in all frames
Number of analysed frames	101
Digital anemometer	Wintact WtT87

The FFT correlation model implies using less computational power while providing a larger sample rate than the DC (direct correlation) model.

A short description of the FFT model is provided by [9] and states that if an FFT is applied to a 2D discrete set of data, the correlation function can be described as  $\mathcal{O}(2N^2 \log_2 N)$ , where  $N$  represents the number of evaluation points and operations. The equation obtained for the FFT can generically be described as  $\mathcal{O}(2N^2 \log_2 N)$ , and presents a reduction factor for the needed operation steps. For example, if  $N=32$ , the number of operations conducted are reduced by  $256/3$ , when compared to the direct correlation  $\mathcal{O}(N^4)$ .

The resulted map of the elements' mediated displacement vectors is illustrated in Figure 4.

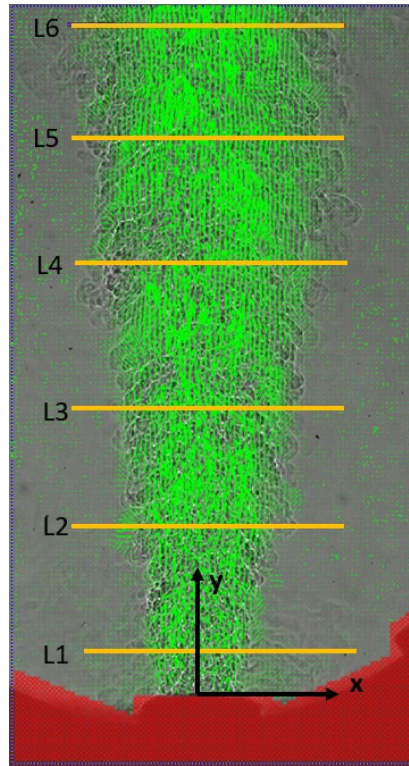


Fig. 4 Map of averaged displacement vectors of the hot-air, turbulent jet, as resulted from PIVlab data processing session, with the horizontal control lines

After obtaining the map of displacement vectors, the velocity profiles are calculated by introducing/entering a calibration image into the program. This calibration image is usually the image of a graded element, placed into the testing area, in the portion which will be covered later by the image of the investigated phenomenon. The magnification factor is then obtained from the length of a gradation element in pixels related to its physical value.

It can already be observed from the vectors' map that the flow contains several parts where it is not covered by displacement vectors. This is due to the elements present in the shear layer, which float around for larger time-periods and are not picked up by the software as their displacement is similar to the displacement of the natural convection elements existing in the background. These vectors are also diminished by the average character of the map.

The next parameters provided by the software are the vorticity map, the jet's streamlines and the sample shear rate, pictured in Figure 5. Figure 5 contains graphic descriptions of the parameters, according to the resulting vectors. The red area contained by the images represents

the mask used to block the program from post-processing the entire image and the forming of spurious vectors from any unwanted reflections produced by the optical system.

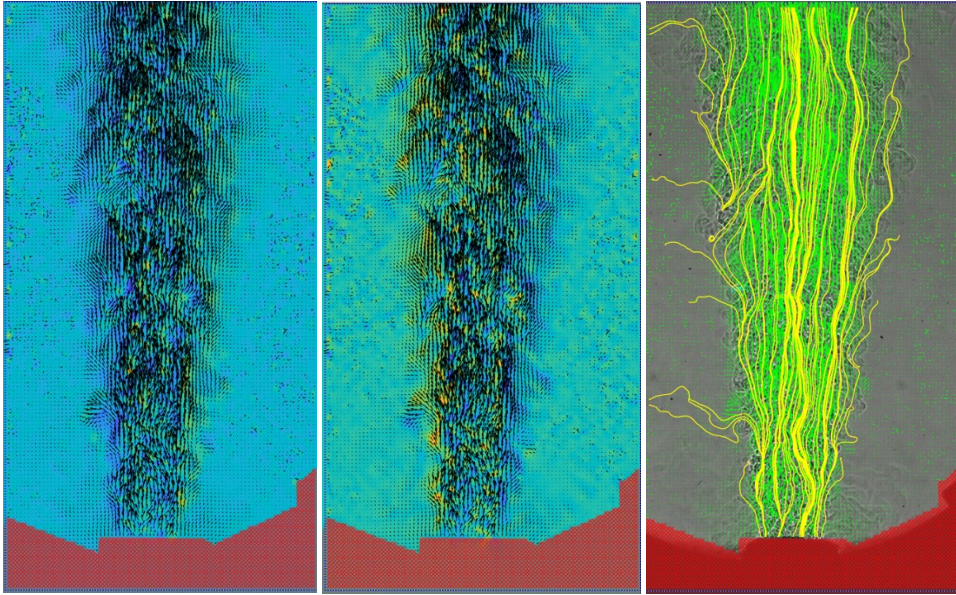


Fig. 5 Vorticity of the hot-air jet(left) and sample shear rate graphic contour (middle) and jet's streamlines (right), as resulted from PIVlab

The velocity profiles are presented as graphical models in Figure 6.

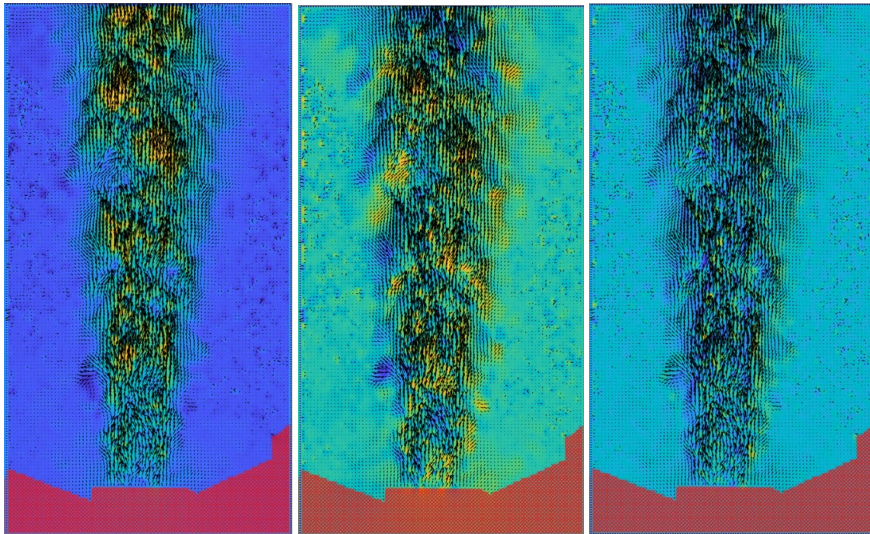


Fig. 6 Velocity profiles of the jet, as resulted from the PIVlab session: (left) V-component, (middle) U-component, (right) velocity magnitude

For further analyze the jet's velocity profiles, 6 horizontal control lines have been placed along the turbulent jet. These are intended to analyze the evolution of the jet's velocity at different distances from the hot air gun's exit nozzle.

The control lines are placed at the following distances from the nozzle of the hot air gun: 10mm, 31mm, 52mm, 74mm, 92mm, and 120mm.

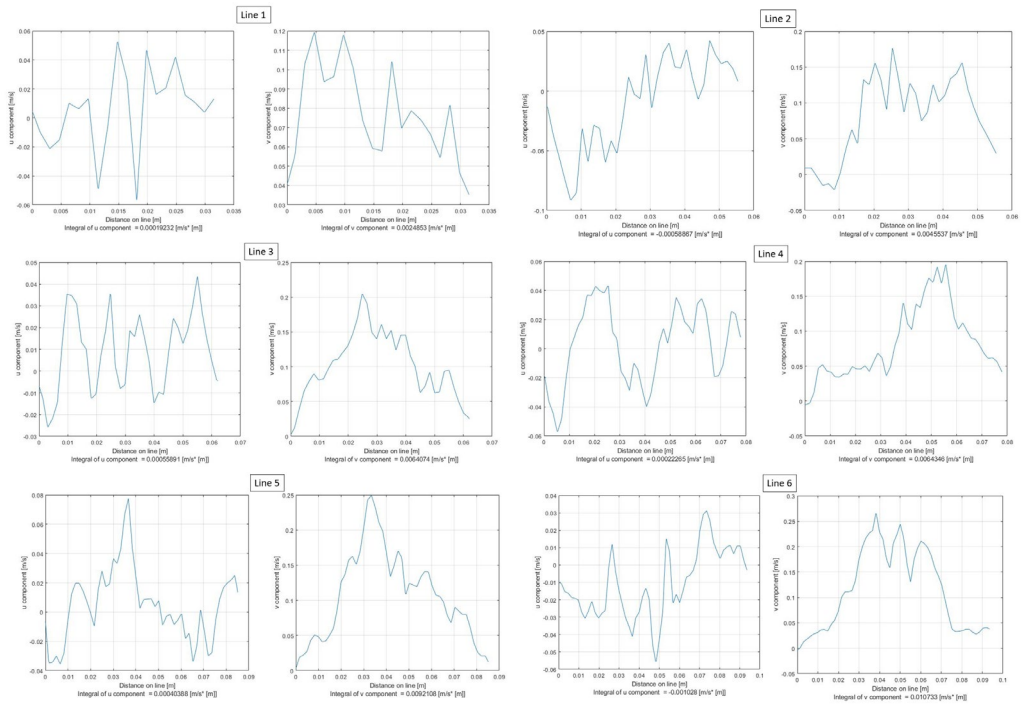


Fig. 7 U and V velocity profiles as resulted from the PIVlab analysis, along the jet’s horizontal control lines

Given the path-integrated character/nature of the flow, the flow velocity is faulty in the area between the nozzle exit and line 3. The explanation is that the program follows the outer elements of the flow, which mix with the surrounding air and tend to linger longer than the interior /inside of the jet. An accuracy map of the method can be found in Figure 8. The values of the global flow velocity are averaged and compared to measurements provided by a digital anemometer placed at the distance indicated by the control lines.

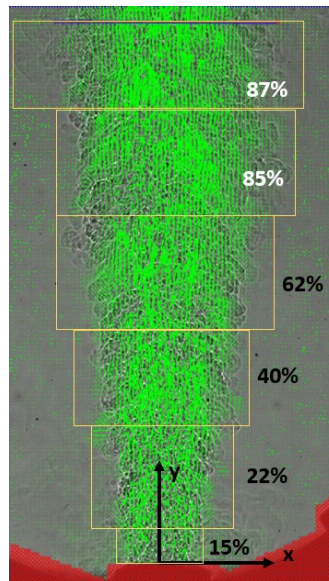


Fig. 8 Accuracy map of the method, per regions limited by the horizontal control lines

The second method applied to the jet is the kymograph method, first used by Settles and Liberzon [4] to find the profile of the center axis velocity. The profile is obtained by processing a batch of 101 images with the ImageJ software [10]. The kymogram of the jet is obtained by opening the image batch in the software, drawing a 1-pixel width line across the jet and using the *KymoReslice* plugin. This results in an image containing 101 1-pixel center lines from each image sequence. This image is called a kymogram, because it contains the velocity curves of the turbulent elements, much like a kymograph registers the pulse wave. The present jet's kymogram can be found in Figure 9.

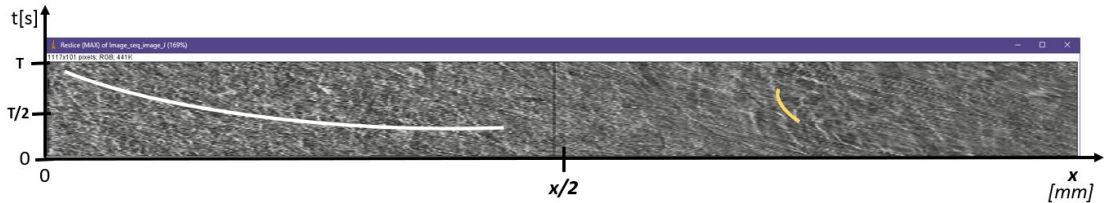


Fig. 9 Kymogram of the turbulent jet, with: white line- the identified central axis velocity, yellow line: turbulent element with a higher slope curve

In the kymograph above, the white line represents the central axis velocity. Unfortunately, it couldn't be tracked for the entire jet, as around the control line number 3, the elements start dispersing at a lower rate. The kymogram also contains a vertical line, representing the constant appearance of a mirror defect. The central axis velocity is calculated by fitting a segment to the image and calculating  $dx/dt$  for each point.

This analysis has been compared to the data recorded by the digital anemometer and the resulting graphs are illustrated in Figure 10.

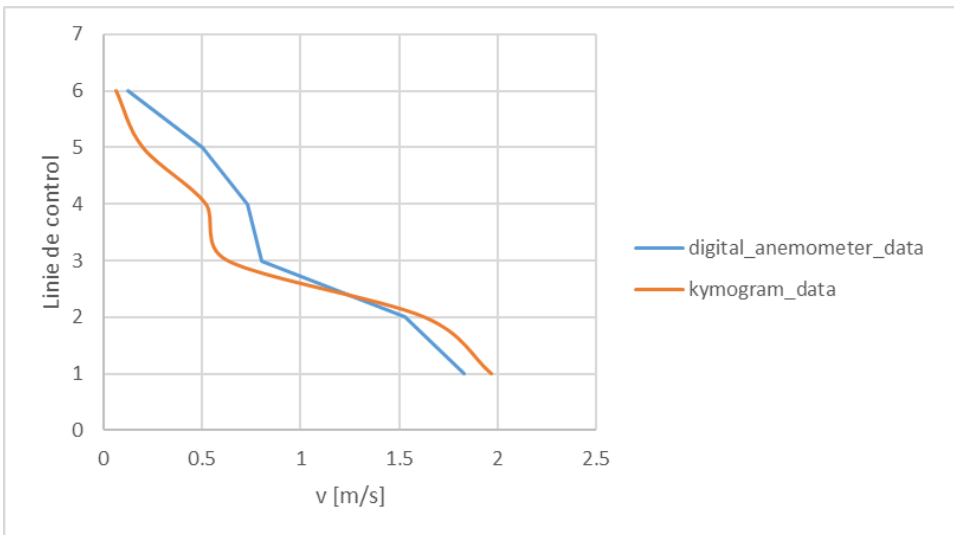


Fig. 10 Results from the kymograph method versus the data recorded by the digital anemometer on the horizontal control lines

#### 4. CONCLUSIONS

The methods presented here offer a reliable result for different areas of the hot, turbulent jet. The PIVlab session is reliable in the jet plumes, offering a velocity accuracy of 87% in the



upper visual limit of the experiment. The accuracy of this method can be improved by performing different analyses for each jet area, and modifying the working parameters of the software to account for the expected values of the jet. The data obtained by FFT cross-correlation does not give a good central-axis velocity profile. This is due to the path-averaged character of the 3D jet, as also found by Fu [11] and Wu [12].

The kymograph method presents a very good accuracy, despite the issues regarding the central axis velocity curve fitting which requires additional image post-processing methods. The first value in the kymograph renders a value slightly higher than the one recorded by the digital anemometer. This can be due to the fact that the curve's first point is mistakenly chosen by the post-processing algorithm or it may be because the values presented by the anemometer are mediated/ averaged, whilst the kymograph is true to the measured flow field. The kymograph method has the disadvantage of presenting data scarcity, as the method assigns one pixel to each measurement point.

Overall, the characterization of the velocity fields of the turbulent hot jet can be achieved within a certain error and can provide a clear interval in which the velocity values are situated. The method is recommended if the desired result is a quick analysis of a flow field without using intrusive and expensive hot wires which can easily lose calibration or suffer physical integrity damage.

## REFERENCES

- [1] E. G. Prisăcariu, T. Prisecaru, R. E. Nicoară, J. A. Vilag, V. A. Vilag, Velocity mapping of an H<sub>2</sub>-O<sub>2</sub> exhaust jet in air, by means of Schlieren Image Velocimetry (SIV), *Aerospace*, vol. **10**(7), 2023.
- [2] S. Biswas, *Physics of Turbulent Jet Ignition*, Cham, Switzerland, Springer International Publishing AG (part of Springer Nature), 2018.
- [3] R. Morales, *Lagrangian Schlieren Image Velocimetry Measurements in Exhaust Plumes, Partial Report*, Master's Thesis, New Mexico Institute of Mining and Technology, Socorro, New Mexico, 2018.
- [4] G. Settles, A. Liberzon, Schlieren and BOS velocimetry of a round turbulent helium jet in air, *Opt. Lasers Eng.*, vol. **156**, 2022, pp. 104-107.
- [5] W. Thielicke, R. Sonntag, Particle Image Velocimetry for MATLAB: Accuracy and enhanced algorithms in PIVlab, in *Journal of Open Research Software*, 2021.
- [6] E. G. Prisăcariu, SIV for an RTJ, using a PIV commercially available post-processing software, *Turbo Journal*, vol. **10**, nr. 1, 2023, pp. 25-45.
- [7] G. Settles, *Schlieren and Shadowgraph Techniques*, Berlin Heidelberg: Springer-Verlag, 2001.
- [8] X. Liu, X. Wang, X. Zhao, P. Xiao, Y. Liu, J. He, An improved inversion algorithm to reconstruct 2D temperature fields of long sparks with high-speed schlieren technique, *Measurement*, 2021.
- [9] M. Bastiaans et al., Cross-correlation PIV: theory, implementation and accuracy, *EUT reports*, vol. **99**, Technische Universiteit of Eindhoven Press, 1993.
- [10] C. A. Schneider, W. S. Rasband, K. W. Eliceiri, NIH Image to ImageJ: 25 years of image analysis, *Nat. Methods* 2012, 9, 671–675.
- [11] Y. Fu, S. Wu, Quantitative analysis of velocity distribution from schlieren images, In *Proceedings of the 8th International Symposium on Flow Visualization*, Sorrento, Italy, 1–4 September 1998, [Google Scholar].
- [12] Y. Wu, Detection of velocity distribution of a flow field using sequences of schlieren images, *Opt. Eng.* 2001, vol **40**.